

Detecting nonlinearity in structural systems using the transfer entropy

J. M. Nichols,* M. Seaver, and S. T. Trickey

U. S. Naval Research Laboratory, Code 5673, Washington, D.C. 20375, USA

M. D. Todd, C. Olson, and L. Overbey

Department of Structural Engineering, University of California San Diego, La Jolla, California 92093-0085, USA

(Received 5 April 2005; published 24 October 2005)

The transfer entropy was recently proposed as a means of exploring coupling in dynamical systems. Transfer entropy is an information theoretic that quantifies the degree to which one dynamical process affects the transition probabilities (dynamics) of another. Here we demonstrate how this metric may be utilized to detect the presence of nonlinearity in a system. Using the method of surrogate data, the transfer entropy computed at various lag times are compared to values computed from linearized surrogates. The transfer entropy is shown to be a more sensitive indicator of nonlinearity than is the mutual information for both simulated and experimental data. This technique is particularly applicable to the field of structural health monitoring, where damage is often equated with the presence of a nonlinearity in an otherwise linear system.

DOI: [10.1103/PhysRevE.72.046217](https://doi.org/10.1103/PhysRevE.72.046217)

PACS number(s): 05.45.Tp, 02.50.Fz

I. INTRODUCTION

In problems of system identification the practitioner is often interested in discerning whether or not the dynamics of an observed system may be appropriately modeled as linear. For example, in the analysis of structural vibration many techniques are based on the assumed linearity of the underlying dynamics, e.g., the eigensystem realization algorithm, complex exponential algorithm, Pisarenko's harmonic decomposition, etc. (see Fahey [1] for a summary). The validity of a linear approximation is also of interest in the field of structural health monitoring (SHM), where structural damage often manifests itself as the introduction of a nonlinearity into an otherwise linear system. Examples include post-buckled structures (Duffing nonlinearity), rattling joints (impacting system with discontinuities), or breathing cracks (bilinear stiffness model). Methods that can reliably quantify the degree of nonlinearity in system dynamics are therefore well suited to the damage detection problem.

The question is more appropriately stated, "Are the observed dynamics consistent with the hypothesis of a linear stochastic process"? A number of researchers have approached this question using the notion of "linearized" surrogate data sets. The surrogate data are designed such that they retain the linear correlations among the original data yet are random with respect to higher order (nonlinear) correlations. Using an appropriate algorithm, data and surrogates are processed, and differences in the results are attributed to nonlinearity. To this end, the mutual information (or its higher dimensional analog, redundancy) is often used as the algorithm of choice. Redundancies represent a probabilistic description of coupling among system components and therefore may be used to capture both linear and nonlinear

relationships. This redundancy-based approach to detecting nonlinearity has been used in a number of studies (see, for example, Paluš [2,3]). The drawback to exploring dynamical relationships with redundancies is that they define coupling in terms of statistical dependencies when what we are often concerned with are dynamical dependencies. This important distinction was noted by Schreiber [4] who suggested a new measure, the transfer entropy, that defines coupling as the degree of influence one system has on another's transition probabilities (dynamics). Later, in Kaiser and Schreiber [5], the transfer entropy was demonstrated to more appropriately quantify the dynamical relationship among time series data than was the mutual information. In particular, the transfer entropy was able to capture asymmetries in the way information was shared between two different dynamical processes.

Because the transfer entropy better captures dynamical dependencies, it seems reasonable to suppose that this metric might be better suited to detecting the presence of nonlinearity in system dynamics than the mutual information. In this work we evaluate the transfer entropy over a range of time scales for both simulated and experimental data where nonlinearity (due to structural damage) is present. We then compare the values of the transfer entropy obtained from these data to those obtained from linear surrogate data. Differences in the results are attributed to the presence of nonlinearity and are quantified using an appropriate index. Both simulated and experimental results suggest that the transfer entropy is more sensitive to nonlinearity in the data than is the time-delayed mutual information function. One may thus hypothesize that transfer entropy is a very useful tool that has a novel application in SHM, where detecting damage is of prime importance.

II. QUANTIFYING DYNAMICAL DEPENDENCE

Let $x_i(n)$ be a time series of the i th system response variable recorded at discrete time n . Furthermore, let $p(x_i)$, $p(x_j)$,

*Email address: pele@ccs.nrl.navy.mil

and $p(x_i, x_j)$ be the single and joint probability densities associated with variables $x_i(n)$ and $x_j(n)$. Mutual information measures statistical independence as $I(x_i; x_j) = \iint p(x_i, x_j) \log_2 [p(x_i, x_j) / (p(x_i)p(x_j))] dx_i dx_j$. For statistically independent distributions the joint density factors [i.e., $p(x_i, x_j) = p(x_i)p(x_j)$] and the mutual information will be zero. Should there exist statistical dependencies, $I(x_i; x_j)$ will be a positive value. Adding a time delay to one of the variables allows for temporal correlations to be accounted for [6]. Letting $p(x_i, x_j(T))$ be the joint density associated with the vectors $x_i(n)$ and $x_j(n+T)$, the time-delayed mutual information is given by

$$I(x_i; x_j, T) = \iint p(x_i, x_j(T)) \log_2 \frac{p(x_i, x_j(T))}{p(x_i)p(x_j(T))} dx_i dx_j(T). \quad (1)$$

Note we have assumed $p(x_j(T)) \approx p(x_j)$, i.e., time-shifting does not alter the individual densities, only the joint density. Because this measure defines coupling in terms of the entire probability density function (as opposed to just covariance properties), it is capable of capturing higher order correlations.

A test for nonlinearity may therefore be designed using the notion of linear surrogate data sets. Given the time series measurements $x_i(n)$ and $x_j(n)$, one may construct surrogates that preserve *only* the covariance properties of the original data. This may be accomplished using the procedure outlined by Prichard and Theiler [7], described briefly here. Denoting the complex Fourier transform (FT) of a time series as $X_i(f) = \mathcal{F}(x_i(n))$, the cross-spectral density between two time series is given by $S_{x_i x_j} = |X_i(f)| |X_j(f)| e^{i[\phi_i(f) - \phi_j(f)]}$. By the Wiener-Khinchine theorem, the inverse FT of the cross-spectral density is the linear cross-correlation function, i.e., $R_{x_i x_j} = \mathcal{F}^{-1}(S_{x_i x_j})$. Adding the same random phase $\psi(f)$ to both $\phi_i(f)$ and $\phi_j(f)$ will therefore preserve $S_{x_i x_j}$ and thus $R_{x_i x_j}$. This method does not preserve the original data amplitude distribution; however, in our particular case we are testing against the null hypothesis that the data are linearly correlated Gaussian noise. This stems from the fact that our undamaged structure is a nominally linear system excited by Gaussian noise, and thus the response is expected to be Gaussian. One may therefore construct surrogate time series $\hat{x}_i(n) = \mathcal{F}^{-1}(X_i(f) e^{i\psi(f)})$ and $\hat{x}_j(n) = \mathcal{F}^{-1}(X_j(f) e^{i\psi(f)})$ that exactly match the second-order correlations in the data, but due to the randomization procedure, any higher order correlations have been destroyed. Comparing $I(x_i; x_j, T)$ and $I(\hat{x}_i; \hat{x}_j, T)$ will therefore produce discrepancies if the relationship between $x_i(n)$ and $x_j(n)$ is nonlinear (possesses higher-order correlation).

Transfer entropy can be used in exactly the same fashion. Transfer entropy asks the question, “do the dynamics of one process, say $x_i(n)$, influence the transition probabilities of another process $x_j(n)$ ”? Both processes are assumed to be described by a generalized Markov model of order k_i and k_j , respectively. In other words, the dynamics of $x_i(n)$ obey $p(x_i(n+1) | x_i(n), x_i(n-1), \dots, x_i(n-k_i+1)) = p(x_i(n+1) | x_i(n), x_i(n-1), \dots, x_i(n-k_i))$. The formulation for trans-

fer entropy given in Ref. [5] allows for the practitioner to choose the order of the governing Markov processes for both $x_i(n)$ and $x_j(n)$. Here we focus on first order processes only such that $k_i = k_j = 1$. The goal in this work is not to build an accurate predictive model of the dynamics, but to simply discern whether or not the dynamics are linear. For this purpose the first order assumption appears to suffice; however, more accurate models may produce better discrimination. For simplicity we will denote $p(x_i(n+1) | x_i(n)) \equiv p(x_i(1) | x_i)$ (dropping the redundant time index “ n ” for notational convenience). If the dynamics $x_j(n)$ are influencing those associated with $x_i(n)$, we have $p(x_i(1) | x_i(n), x_j(n)) \neq p(x_i(1) | x_i(n))$. The degree of influence may therefore be mapped onto a scalar via the transfer entropy

$$\begin{aligned} \text{TE}(x_i(1) | x_i, x_j) \\ = \iint \iint p(x_i(1), x_i, x_j) \log_2 \frac{p(x_i(1) | x_i, x_j)}{p(x_i(1) | x_i)} dx_i(1) dx_i dx_j. \end{aligned} \quad (2)$$

Similar to the mutual information, a null hypothesis is placed in the denominator of the logarithm (assumption of independence) while the alternative hypothesis resides in the numerator. Because Eq. (2) is naturally nonsymmetric in its arguments, there is no need to introduce a time delay to assess directionality of information flow. However, we find that it is still useful to introduce such a delay allowing one to quantify the information carried in $x_j(n+T)$ about the transition probabilities $p(x_i(1) | x_i)$. We are therefore still considering a first order Markov model of the dynamics, but are considering the influence of the second time series across a variety of time scales. It is reasonable to assume, for example, that the value $x_j(n-20)$, for example, carries added information about the transition from $x_i(n) \rightarrow x_i(n+1)$. This information is more formally obtained by simply increasing the order of the assumed Markov model, e.g., $k_j = 20$; however, there is a computational cost associated with the estimation of the transfer entropy in higher-dimensional space (see Sec. II A). The introduction of a delay, while not necessary to detect asymmetries in the dynamical relationships, is still an appropriate tool for exploring temporal dependencies. It will be shown that not only do these temporal dependencies exist, but they provide valuable information about the dynamics of the underlying processes. We note briefly that values associated with positive delays should not be thought of as influencing past behavior (an impossibility) but rather containing information about past behavior. Only in the case of unidirectional coupling is it necessary to consider only negative (or positive, depending on which signal is the driver) delays. For processes with bidirectional coupling (or where it is not known *a priori* if biased coupling occurs), it makes sense to examine the transfer entropy in both forward and reverse time.

Letting $p(x_i, x_j(T)) \equiv p(x_i(n), x_j(n+T))$ (again dropping time index n for convenience) and expanding Eq. (2) as the sum and difference of various entropies gives

$$\begin{aligned}
 \text{TE}_{x_j \rightarrow x_i} &\equiv \text{TE}(x_i(1)|x_i, x_j(T)) \\
 &= \int \int \int p(x_i(1), x_i, x_j(T)) \\
 &\quad \times \log_2 p(x_i(1), x_i, x_j(T)) dx_i(1) dx_i dx_j(T) \\
 &\quad + \int p(x_i) \log_2 p(x_i) dx_i \\
 &\quad - \int \int p(x_i, x_j(T)) \log_2 p(x_i, x_j(T)) dx_i dx_j(T) \\
 &\quad - \int \int p(x_i(1), x_i) \log_2 p(x_i(1), x_i) dx_i(1) dx_i.
 \end{aligned} \tag{3}$$

Equation (3) will be referred to as the time-delayed transfer entropy and will be shown to be a useful metric in diagnosing the presence of nonlinearity in the coupling between $x_i(n)$ and $x_j(n)$.

A. Estimation from time series

Estimates of the transfer entropy (and redundancies) require approximations of the various entropies that comprise them. It has been shown [8,9] that if a kernel density estimation is performed about *each* point in the time series, the entropies may be approximated by

$$\int p(\mathbf{x}(n)) \log_2 [p(\mathbf{x}(n))] d\mathbf{x} \approx \frac{1}{N} \sum_n \log_2 [\hat{p}(\mathbf{x}(n), \epsilon)], \tag{4}$$

where

$$\hat{p}(\mathbf{x}(n), \epsilon) = \frac{1}{N\epsilon} \sum_m K\left(\frac{|\mathbf{x}(n) - \mathbf{x}(m)|}{\epsilon}\right), \tag{5}$$

and $K(\cdot)$ is the kernel. Here we utilize the familiar ‘‘step’’ kernel [9], such that Eq. (5) becomes

$$\hat{p}(\mathbf{x}(n), \epsilon) = \frac{1}{N - 2t - 1} \sum_{m: |m-n| > t} \Theta(\epsilon - \|\mathbf{x}(n) - \mathbf{x}(m)\|),$$

where $\Theta(\cdot)$ is the Heaviside function and the parameter t is introduced as the Theiler window (chosen to exclude temporally correlated points within t time steps of n from consideration in the estimate). This estimation technique is referred to as a fixed bandwidth approach. We also consider a fixed-mass approach, whereby the number of points used to define the local density remains constant while the bandwidth is allowed to vary. This approach has the advantage of being adaptive; that is, areas of high density occupy smaller vol-

umes and vice versa. For the adaptive kernel, Eq. (5) may be rewritten

$$\hat{p}(\mathbf{x}(n), M) = \frac{1}{N - 2t - 1} \frac{M}{V(\mathbf{x}(n))},$$

where M is a fixed number of nearest neighbors to the fiducial point $\mathbf{x}(n)$, and $V(\mathbf{x}(n))$ is the volume containing these points. This volume may be computed a number of ways; here we use both hyperspheres and hyperrectangles. For the hypersphere volume element, the radius is taken as the Euclidean distance from $\mathbf{x}(n)$ to the furthest of the M near neighbors. For the rectangular elements, the volume element is given by $V(\mathbf{x}(n)) = \prod_j \epsilon_j$, where the ϵ_j are the sides of the smallest enclosing rectangle associated with the M points. The constituent entropies for both mutual information and transfer entropy are again computed via Eq. (4). It should be noted that the fixed mass approach is much more computationally intensive than the fixed bandwidth approach. Finding the M nearest neighbors in a data space is inherently more difficult than finding all neighbors within a given radius. Choice of kernel can be heavily dependent on the nature of the quantity being estimated. The transfer entropy is much more sensitive to choice of kernel than is the mutual information function as will be shown.

B. Information-theoretics for linear structures

In certain instances both time-delayed mutual information and time-delayed transfer entropy admit analytical solutions. The dynamics of a linear, dissipative, Gaussian-excited structure obey

$$\mathbf{M}\{\ddot{\mathbf{x}}\} + \mathbf{C}\{\dot{\mathbf{x}}\} + \mathbf{K}\{\mathbf{x}\} = \mathbf{f}(t), \tag{6}$$

where $\mathbf{M}, \mathbf{C}, \mathbf{K}$ represent, respectively, the $L \times L$ constant-coefficient mass, damping, and stiffness matrices of the L degree-of-freedom structure. Let \mathbf{u}_i be the nontrivial eigenvector(s) of the associated Hamiltonian eigenvalue problem $|\mathbf{K} - \omega^2 \mathbf{M}| \mathbf{u}_i = \mathbf{0}$. Furthermore let these eigenvectors (known as mode shapes) be ‘‘mass normalized’’ such that $\mathbf{u}_i^T \mathbf{M} \cdot \mathbf{u}_i = I$ (the identity matrix). If the Gaussian excitation is applied to the end mass the forcing vector is written $\mathbf{f}(t) = [0, 0, \dots, \mathcal{N}(0, 1)]^T$. Because the structure is linear, the response of any of the L degrees of freedom will also be Gaussian, and the linear cross-correlation between any two state variables x_i and x_j is given by

$$\begin{aligned}
 R_{x_i x_j}(\tau) &= \frac{1}{4} \sum_l^L \sum_m^L u_{Ll} u_{Lm} u_{il} u_{jm} [A_{lm} e^{-\zeta_m \omega_m \tau} \cos(\omega_{dm} \tau) \\
 &\quad + B_{lm} e^{-\zeta_m \omega_m \tau} \sin(\omega_{dm} \tau)],
 \end{aligned} \tag{7}$$

where

$$A_{lm} = \frac{8(\omega_l \zeta_l + \omega_m \zeta_m)}{\omega_l^4 + \omega_m^4 + 4\omega_l^3 \omega_m \zeta_l \zeta_m + 4\omega_m^3 \omega_l \zeta_l \zeta_m + 2\omega_m^2 \omega_l^2 (-1 + 2\zeta_l^2 + 2\zeta_m^2)},$$

$$B_{lm} = \frac{4[\omega_l^2 + 2\omega_l\omega_m\zeta_l\zeta_m + \omega_m^2(-1 + 2\zeta_m^2)]}{\omega_{dm}[\omega_l^4 + \omega_m^4 + 4\omega_l^3\omega_m\zeta_l\zeta_m + 4\omega_m^3\omega_l\zeta_l\zeta_m + 2\omega_m^2\omega_l^2(-1 + 2\zeta_l^2 + 2\zeta_m^2)]}. \quad (8)$$

This derivation assumes that the damping matrix \mathbf{C} is diagonalizable, achieved through a modal damping model with dimensionless damping ratios ζ_i defining the fraction of critical (required for oscillatory behavior) damping in the i th mode. The damped natural frequencies are therefore given by $\omega_{di} = \sqrt{1 - \zeta_i^2}\omega_i$. The linear cross-correlation coefficient is obtained from Eq. (7) through the normalization

$$\rho_{x_i x_j}(T) = R_{x_i x_j}(T) / \sqrt{R_{x_i x_i}(0)R_{x_j x_j}(0)}. \quad (9)$$

For linear structures, a closed form expression for both time-delayed mutual information and time-delayed transfer entropy may be obtained by carrying out the integration required in Eqs. (1) and (3), respectively, resulting in

$$I(x_i; x_j, T) = -\frac{1}{2} \log_2 [1 - \rho_{x_i x_j}^2(T)],$$

$$\text{TE}(x_i(1)|x_i, x_j(T)) = \frac{1}{2} \log_2 \frac{[1 - \rho_{x_i x_j}^2(T)][\hat{R}_{x_i x_i}^2(1) - 1]}{-2\rho_{x_i x_j}(T-1)\hat{R}_{x_i x_i}(1)\rho_{x_i x_j}(T) + \rho_{x_i x_j}^2(T-1) + \{\hat{R}_{x_i x_i}^2(1) + [-1 + \rho_{x_i x_j}^2(T)]\}}, \quad (10)$$

where we have denoted $\hat{R}_{x_i x_i}(T) = R_{x_i x_i}(T)/R_{x_i x_i}(0)$ as the normalized autocorrelation. As expected, the linearized mutual information function is a function of only the linear cross-correlation between $x_i(n)$ and $x_j(n)$. For time-delayed transfer entropy the formula is slightly more complicated and includes both autocorrelations and cross-correlations as well as time-shifted versions of both quantities. The appearance of autocorrelation terms stems from the transition probabilities $p(x_i(1)|x_i)$, while the time-shifted cross-correlation terms result from the covariance between $x_i(n+1)$ and x_j . Both numerator and denominator of the linearized transfer entropy are very small in magnitude [$O(10^{-3})$ for this numerical example], as they contain terms that scale with the derivatives of the linear autocorrelation and cross-correlation functions, i.e., $\rho_{x_i x_j}^2 - 1$ and $\hat{R}_{x_i x_i}^2 - 1$. The result is a metric that is inherently more sensitive to changes in the dynamics of structural systems than is the mutual information function. Equation (10), combined with Eqs. (7)–(9), provides an analytical solution for assessing the various kernel density estimation schemes.

Both fixed bandwidth and fixed mass approaches were considered in this work. Using the simulated displacements, consisting of $N=2^{16}$ points, for masses 2 and 3 both the transfer entropy and mutual information were computed and compared to their theoretical values. For the time-delayed mutual information all approaches to estimation gave good quantitative agreement (see Fig. 1, left). This particular metric is largely insensitive to the type of density estimation and the parameter values used ϵ, M . Here we show results for $\epsilon=0.05$, $M=10$. Furthermore, only $I(x_3; x_2, T)$ is shown as $I(x_2; x_3, T)$ is nearly identical, the only difference being a slight translation moving the center peak from $T>0$ to

$T<0$. The transfer entropy metric proved more challenging to estimate. Using the fixed bandwidth approach yields values for $T_{3 \rightarrow 2}$ that shows qualitative agreement only to the theoretical curve. A number of different ϵ values were used, each one showing significant deviations from theory (the value used in the figure, $\epsilon=0.05$ gave the best estimate). The fixed-mass approaches performed significantly better showing good quantitative agreement to theory. Estimates using both hyperrectangles and hyperspheres were performed and the results displayed in the right two plots of Fig. 1. For the transfer entropy both $T_{3 \rightarrow 2}$ and $T_{2 \rightarrow 3}$ are shown as there exists a significant difference in the results. By design, the transfer entropy metric is able to capture asymmetries in the flow of information. The differences in the curves therefore pertain directly to which end of the structure is being forced. This information is difficult to extract from the mutual information function. We now demonstrate how the time-delayed transfer entropy, in conjunction with surrogate data, can be used to outperform mutual information in detecting the presence of a structural nonlinearity

III. SIMULATED STRUCTURE WITH QUADRATIC STIFFNESS NONLINEARITY

As a first step we considered the model Eq. (6) with “fixed-free” boundary conditions and included a quadratic nonlinearity in the stiffness matrix, i.e., $\mathbf{K}=\mathbf{K}(\mathbf{x})$. Specifically, we allow the force of coupling between masses 2 and 3 to include both linear and nonlinear components. The restoring force (itself cubic in nature due to the quadratic nonlinearity) generated by the system stiffness may be written more compactly in terms of relative mass displacements as

$$\underbrace{\begin{bmatrix} k_1 & -k_2 & 0 & 0 & 0 \\ 0 & k_2 & -k_3(1-\mu(x_3-x_2)^2) & 0 & 0 \\ 0 & 0 & k_3(1-\mu(x_3-x_2)^2) & -k_4 & 0 \\ 0 & 0 & 0 & k_4 & -k_5 \\ 0 & 0 & 0 & 0 & k_5 \end{bmatrix}}_{\mathbf{K}(x)} \underbrace{\begin{bmatrix} x_1 \\ x_2 - x_1 \\ x_3 - x_2 \\ x_4 - x_3 \\ x_5 - x_4 \end{bmatrix}}_{\Delta x}$$

Equation (6) was simulated using $\mathbf{M}=\mathbf{I}$ (i.e., all mass values are unity) and $k_i=10.0$ N/m, $i=1, \dots, 5$. The damping matrix \mathbf{C} follows the same form as the linear portion of the stiffness matrix with entries $c_i=0.01$ N s/m, $i=1, \dots, 5$. Gaussian noise of unit standard deviation was used to excite the structure at the end mass (mass 5). Response data were recorded for each of the five mass displacements for $n=1, \dots, 2^{16}$ points for $\mu=0$ (no nonlinearity), and both time-delayed mutual information and time-delayed transfer entropy were computed. Using the FT-based approach, ten linear surrogate data sets were created and both the mutual information and transfer entropy computed for each. In the initial cases we used forty surrogates (a number chosen similarly to previous studies [7,10]) and found no significant changes in results. Therefore ten surrogates were always used for subsequent analyses. This process was repeated for μ increasing from zero up to the bifurcation point where cross-well behavior is observed (resonant jump). At this point, of course, it becomes trivial to detect the nonlinearity. Results comparing data and surrogates are shown in Fig. 2 using the fixed bandwidth approach. These results also highlight the need for examining the transfer entropy over a variety of lags. For zero lag, little difference is observed between the data and the surrogates, while for $T=\pm 2$ a large separation between surrogates and original data is evident. That higher-order correlations are more clearly observed at delays other than $T=0$ is not surprising. For this system, the masses are directly coupled such that for zero lag there is a great deal of redundant information. Regardless of the degree of nonlinearity, the transfer entropy for $T=0$ is always near zero. Positive and/or negative lags are needed to provide additional information about the nature of the underlying model (linear/nonlinear). It is apparent that the transfer entropy provides a greater discernment between data and surrogates over a wider range of time scales thus making it easier to resolve the presence of the nonlinearity.

We also computed results using the fixed mass approach with a variety of mass sizes. The results for $M=20$ are shown in Fig. 3. Again, the transfer entropy shows an increased difference between original and surrogate data however the degree of separation is similar to that achieved using the fixed bandwidth approach. From this preliminary work we therefore conclude that there is no compelling reason to utilize the more time-consuming fixed-mass kernel density estimation approach if the goal is to simply detect the presence of a nonlinearity. Although the fixed mass approach yields a more accurate result, it is not clear that the relative separation between data and surrogates is improved. For this reason we utilize the more efficient fixed-epsilon estimator in the following experimental examples.

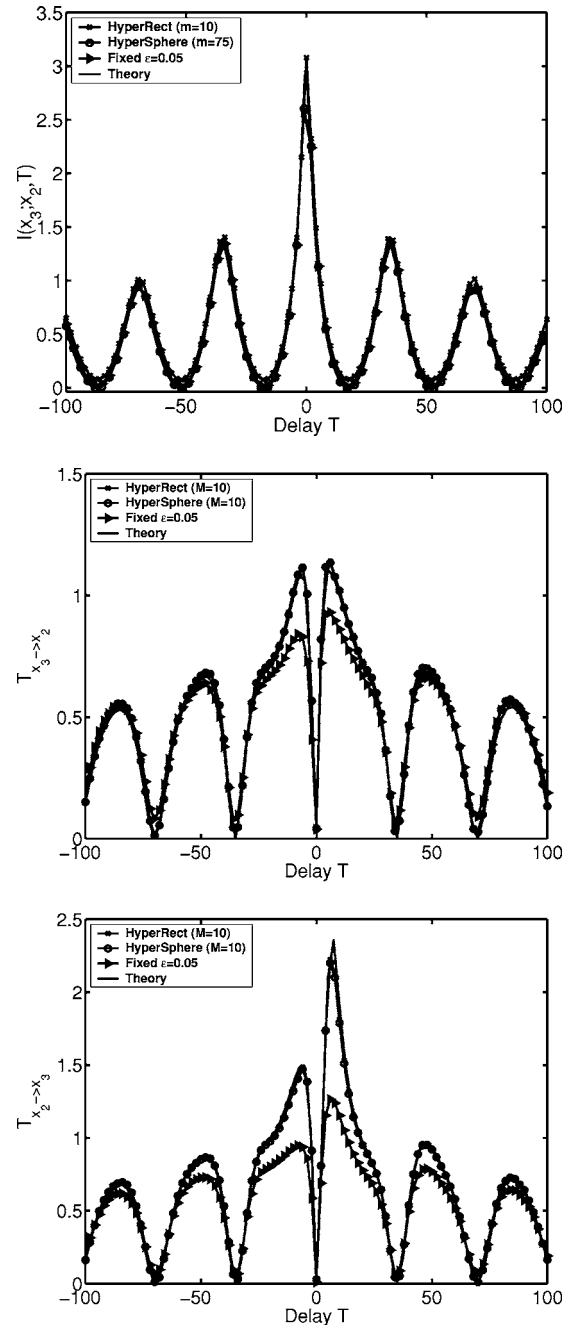


FIG. 1. Comparison of various estimation methods for Mutual Information [$I(x_3; x_2, T)$] (top) and transfer entropy ($T_{x_3 \rightarrow x_2}, T_{x_2 \rightarrow x_3}$) (middle and bottom).

IV. EXPERIMENT 1: LOOSENING OF A BOLTED CONNECTION

In the first experiment, the frame structure shown in Fig. 4 was constructed. The structure was a one-bay stainless-steel frame consisting of two vertical members (12 in \times 2 in \times 0.25 in) and a horizontal member (22 in \times 2 in \times 0.25 in) bolted together with 3.5 in \times 3.5 in \times 0.25 in steel angle brackets. The vertical members were bolted via angle brackets to a 26.75 in \times 8 in \times 0.5 in steel plate which was in turn clamped to a laboratory table in order to simulate a fixed boundary condition.

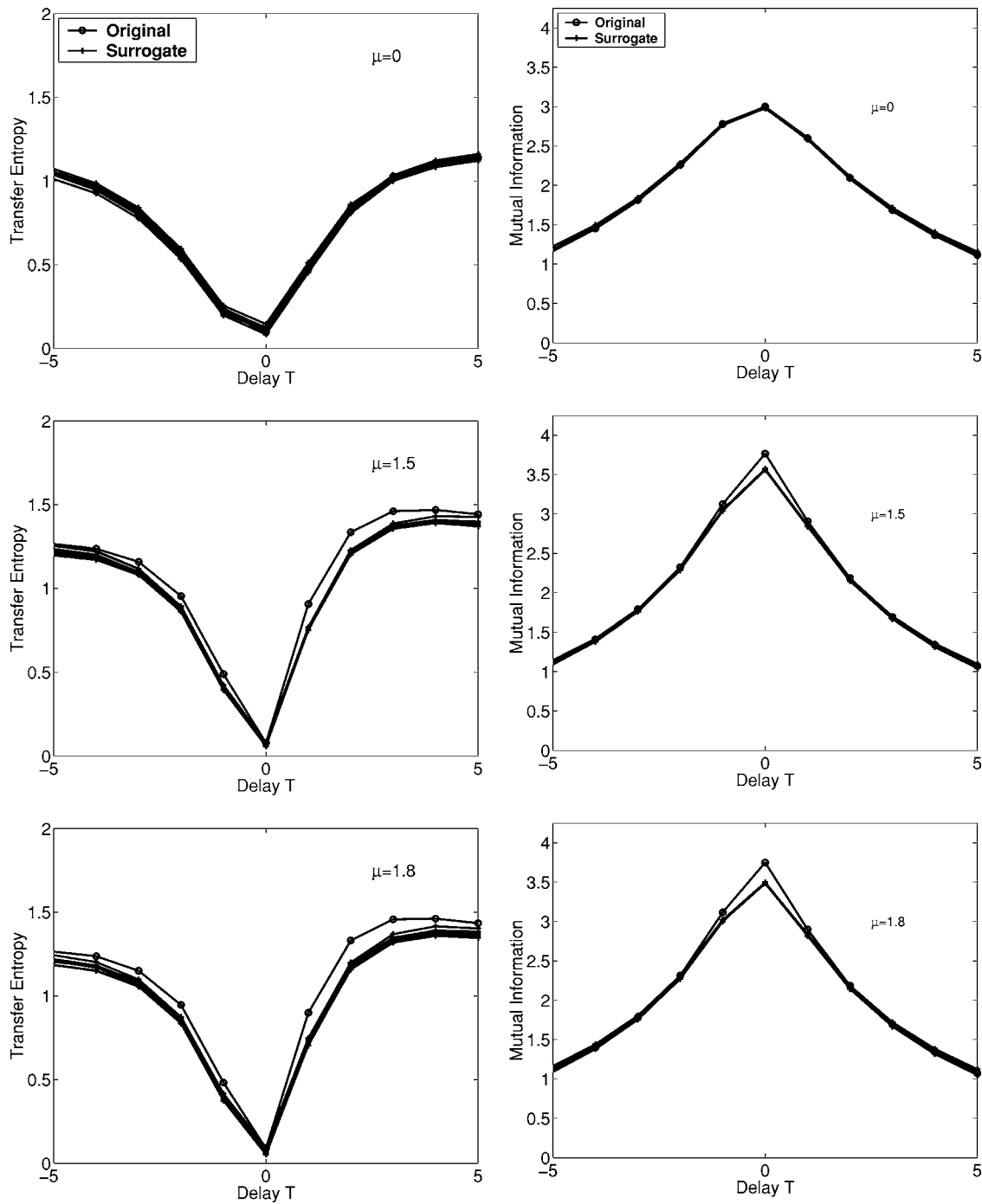


FIG. 2. Transfer entropy and mutual information for surrogates (+) and original data (O) using the fixed bandwidth approach to estimation ($\epsilon=0.1$).

Gaussian noise signals with center frequency near 500 Hz were generated in LabVIEW. The structure was excited with this waveform by a MB Dynamics PM50A shaker clamped to the same table and attached via a stinger to one of the vertical spars. PCB A352C65 ICP accelerometers (100 mV/g) were attached with wax to measure the response at three locations on the structure. These accelerometers were located near one of the brackets connecting the horizontal member to one of the vertical members. One accelerometer was placed below the bolt on the excitation (out-

board) side of the vertical spar (channel 1), the second was placed above the bolt on the horizontal spar (channel 2), while the other was placed above the bolt on the vertical member opposite the excitation (channel 3).

The shaker was powered by a MB Dynamics SL500 VCF power amplifier which in turn was controlled by a National Instruments PCI 6036E D/A card. Excitation control and data acquisition were managed through a National Instruments (NI) LabVIEW 7.0 interface and a NI SCXI-1000 chassis. For each excitation case, a six-second signal was generated

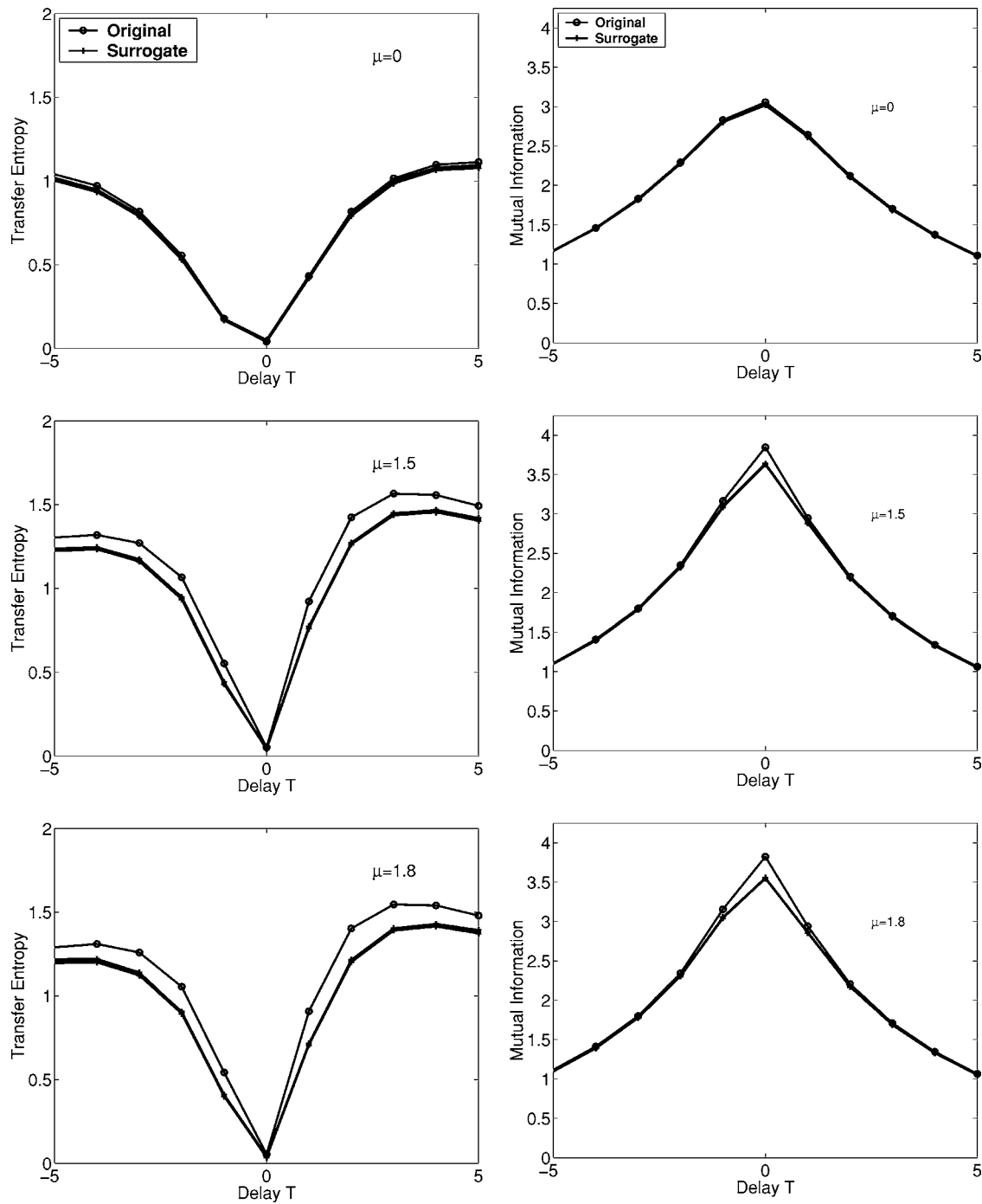


FIG. 3. Transfer entropy and mutual information for surrogates (+) and original data (O) using the fixed mass approach to estimation ($\epsilon=0.1$).

in LabVIEW and sent to the amplifier upon which the accelerometer responses were managed in multiplex by a SCXI-1531 module and read into LabVIEW. The shaker update rate and all data acquisition were performed at 20 kS/s.

Damage was simulated at one of the joints by altering the initial torque of the bolt at that joint. The acceleration response of the structure to the Gaussian input was measured at each damage case. Damage case 0 corresponds to full bolt torque (120 in-lb), damage case 1 to 60 in-lb, damage case 2 to 30 in-lb, damage case 3 to a “finger tight” condition,

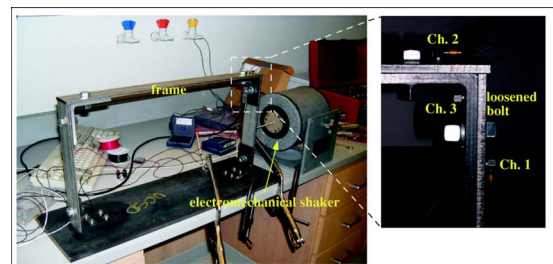


FIG. 4. (Color online) Frame structure with accelerometers located at one joint.

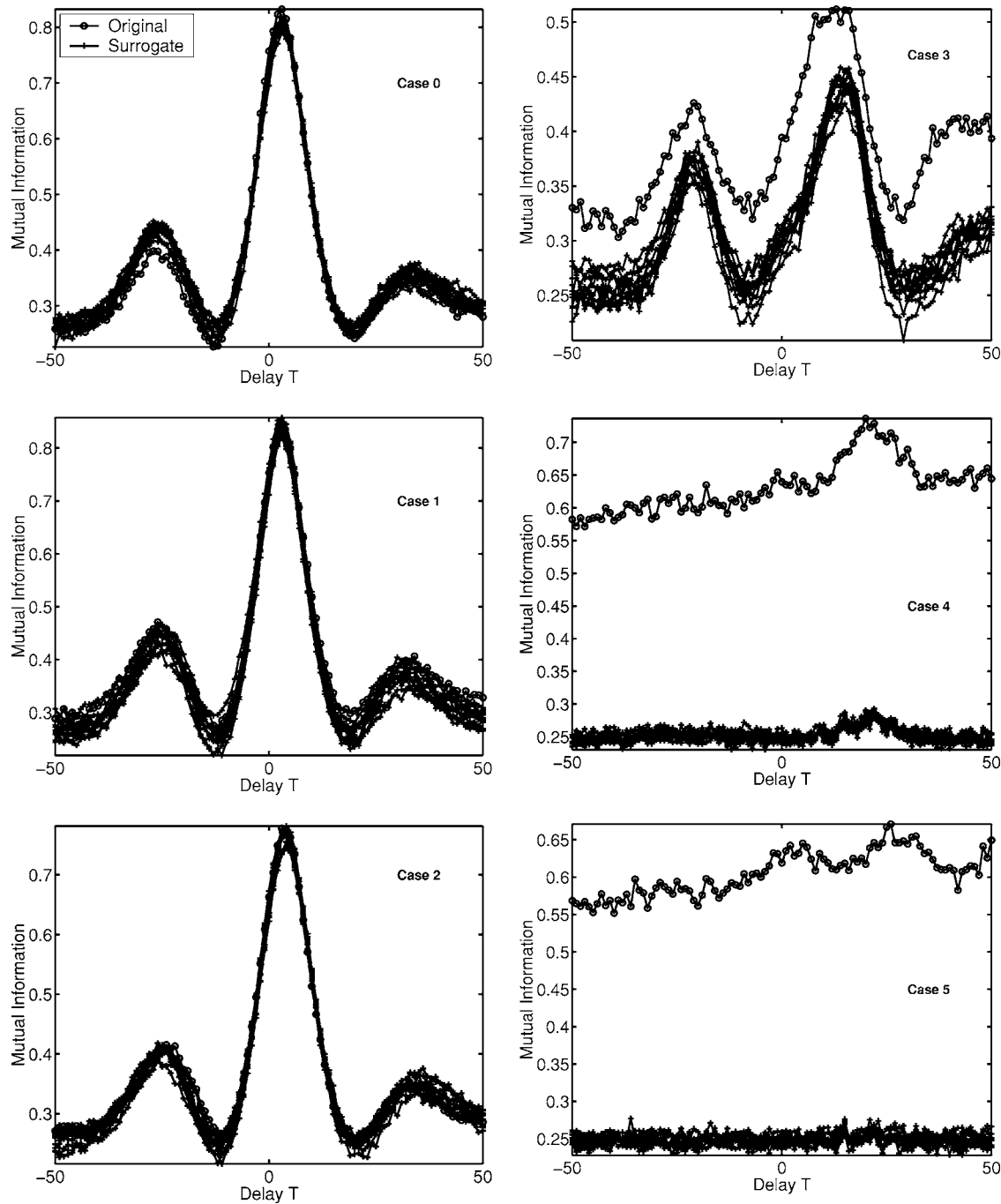


FIG. 5. Mutual information for surrogates (+) and original data (○).

damage case 4 to a “fully loose” condition, and damage case 5 to a completely removed bolt.

Ten linearly related surrogate data sets were generated for this sensor pair. Both the time-delayed mutual information and time-delayed transfer entropy were then computed for both the original data and the surrogates using the fixed-epsilon approach with $\epsilon=0.1$. Results of this computation are shown in Figs. 5 and 6 for each of the six damage cases (including the baseline condition, case 0). While the joint is in the fully tightened condition no difference is observed between the metric values for the data and the surrogates. Under this condition the structure’s dynamics are consistent

with the hypothesis of a linear model. The structure appears to adhere to a linear model until damage case 3 for the mutual information and damage case 2 with the transfer entropy, where in each case separation is observed between the data and the surrogates. The final two damage cases for both metrics show gross differences suggesting a high degree of non-linearity is present. This is expected as a loose joint will exhibit both impact discontinuities and “stick-slip” phenomenon in the dynamics. The differences between data and surrogates may be made explicit by constructing a damage index. At each delay we use the surrogate mean μ_S and standard deviation σ_S to form the metric

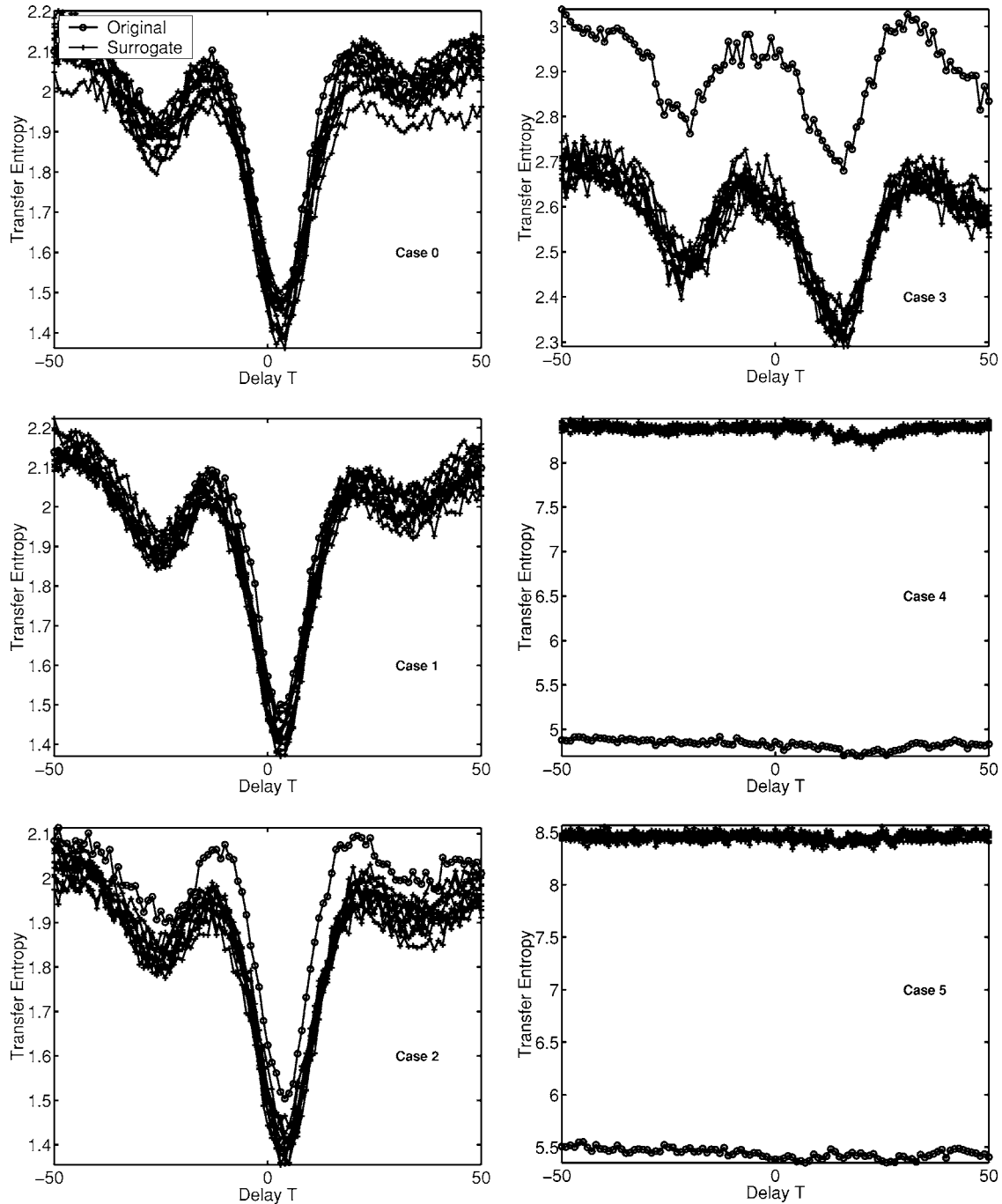


FIG. 6. Transfer entropy for surrogates (+) and original data (○).

$$\xi(T) = \frac{[I(T) \text{ or } TE(T)] - \mu_S}{\sigma_S}$$

using either the mutual information (I) or transfer entropy (TE) computed features. By applying a suitable threshold for significance we may test the hypothesis of linearity at each delay T . Alternatively, we can compare the average normalized metric value $\bar{\xi}(T) = (1/2T) \sum_{-T}^T \xi(T)$ to the threshold. In this work we take the latter approach and form the average normalized metric value and compare to the threshold $S=1.96$ for 95% confidence (assuming the surrogates are

normally distributed). The final damage index is given by the degree to which the threshold is exceeded by taking

$$Z = (\bar{\xi} - S)\Theta(\bar{\xi} - S),$$

where $Z_{I,TE}=0$ for $\bar{\xi} < S$ (threshold is not exceeded). Results are shown in Fig. 7 for both mutual information and transfer entropy. The two metrics clearly show different levels of sensitivity to the damage. Mutual information classifies the dynamics of case 3 as linear whereas the transfer entropy clearly indicates the presence of a nonlinear relationship. The degree to which the average transfer entropy (over all delays)

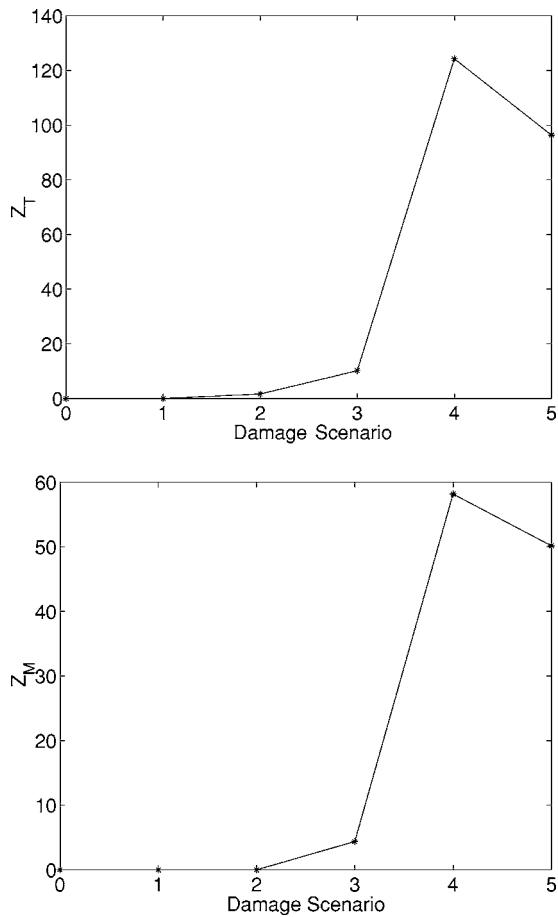


FIG. 7. Damage indices for both mutual information and transfer entropy.

exceeds the confidence limits is much greater than for the mutual information. Thus, the transfer entropy possesses greater sensitivity to structural damage for this particular experiment.

V. EXPERIMENT 2: IMPACT DAMAGE IN COMPOSITE PLATES

In this second example the structure of interest is a thick composite sandwich plate subject to varying levels of impact damage. Three plates were tested, one with no damage, one that was impacted with 672 ft-lb of force at its center, and a third that was impacted with 1344 ft-lb of force, also at the plate center. A picture of the third plate is shown in Fig. 8 with damage located at the center. A series of fiber Bragg-grating strain sensors were mounted on the surface of the plate and were used to record the plate’s strain response. A complete description of this sensing system may be found in Ref. [11]. The plate was excited with broadband (0–200 Hz) Gaussian noise and response data were sampled at a rate of 800 Hz. Both mutual information and transfer entropy were then computed for ten linear surrogates and the original time series. Each sensor pair was analyzed, i.e., we compute $I(x_i; x_j, T)$ and $TE_{j \rightarrow i}$ for $i, j = 1, \dots, 10$ using the fixed bandwidth approach with $\epsilon = 0.1$. Damage indices were then extracted in the same fashion as for the bolted

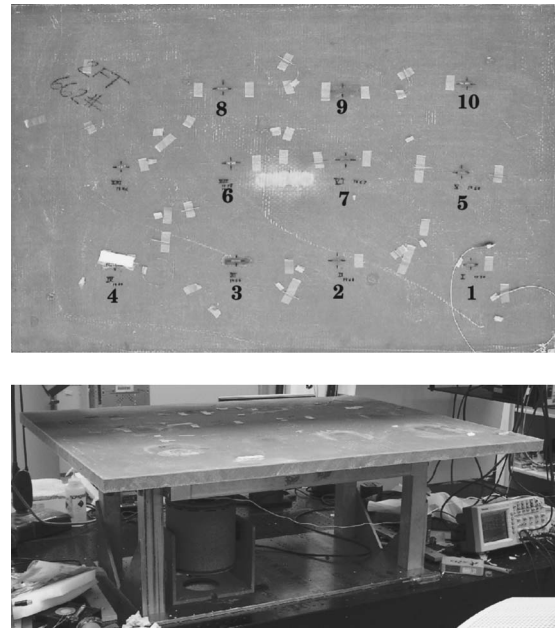


FIG. 8. Damaged composite plate showing sensor locations (left) and experimental setup (right).

joint study and plotted for each sensor pair in Fig. 9. In these plots, darker shading indicates higher levels of nonlinearity, while white is used for zero nonlinearity, as quantified using the aforementioned damage indices. The top row of plots shows the indices obtained using the mutual information function while the bottom row shows results based on the transfer entropy. The transfer entropy is clearly detecting nonlinearity where the mutual information fails to do so. The majority of sensor pairs for plate No. 2 suggest a nonlinear relationship when analyzed with the transfer entropy whereas only a few sensor pair indicate nonlinearity using the time delayed mutual information. Even for the most damaged plate the transfer entropy is clearly able to resolve the presence of the impact. The mutual information function can resolve the presence of the impact on plate No. 3 only.

The indication for both this and the previous experiment is that the transfer entropy is better suited to detecting the presence of nonlinearity in structural dynamics. This heightened sensitivity is likely due to the fact that the transfer entropy is a more appropriate definition of dynamical coupling than is the mutual information. Rather than analyzing statistical dependencies as a function of delay, the transfer entropy focuses on transition probabilities, thus dynamical dependencies, directly. We thus believe that the inclusion of dynamics in the definition of coupling (such as with transfer entropy) increases sensitivity to the form of the dynamics (linear or nonlinear).

VI. CONCLUSIONS

We explored the time-delayed transfer entropy as an effective metric for assessing the degree of nonlinearity present in a system’s dynamics, and we compared to the use of time-delayed mutual information for the same purpose. For linear

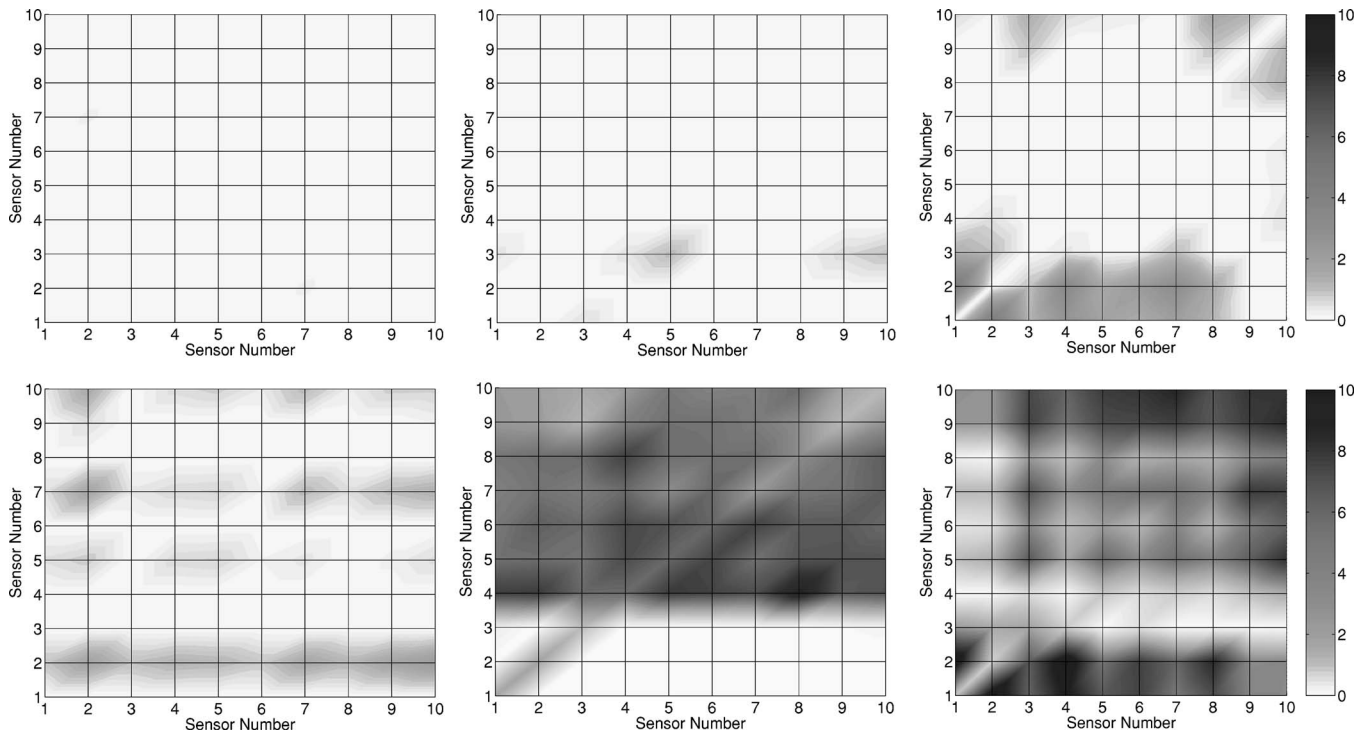


FIG. 9. Damage indices recorded for plates 1, 2, and 3 (left to right) using mutual information (top row) and transfer entropy (bottom row) for all sensor pairs.

structural systems, we presented a general analytical solution and compared estimates of the transfer entropy using several different kernel density approaches. We found that a fixed mass approach produces the most accurate estimate, although computation time is significantly increased. We then used this metric in combination with linear surrogate data to deduce the degree of nonlinearity in both simulated and experimental structures subject to increasing nonlinearity from damage. Based on the simulation results, we concluded that, at least for this application, the fixed bandwidth estimator performs as well as the fixed mass estimator. Furthermore,

both simulation and experiment suggest that the transfer entropy appears to be more sensitive to nonlinear coupling among a structure's components than is the mutual information (which is more commonly used). This sensitivity is attributed to the effect the transfer entropy is designed to capture, namely, the influence of one signal's dynamics on the transition probabilities of the other. We conclude that transfer entropy is a useful tool applied to nonlinearity detection problems in structural health monitoring, where the goal is to detect damage in the structure from an observed vibration measurement.

-
- [1] S. Fahey and J. Pratt, *Exp. Tech.* **22**, 45 (1998).
 [2] M. Paluš, *Physica D* **80**, 186 (1995).
 [3] M. Paluš, V. Komarek, Z. Hrnčíř, and K. Sterbova, *Phys. Rev. E* **63**, 046211 (2001).
 [4] T. Schreiber, *Phys. Rev. Lett.* **85**, 461 (2000).
 [5] A. Kaiser and T. Schreiber, *Physica D* **166**, 43 (2002).
 [6] J. A. Vastano and H. L. Swinney, *Phys. Rev. Lett.* **60**, 1773

- (1988).
 [7] D. Prichard and J. Theiler, *Phys. Rev. Lett.* **73**, 951 (1994).
 [8] W. Liebert and H. G. Schuster, *Phys. Lett. A* **142**, 107 (1989).
 [9] D. Prichard and J. Theiler, *Physica D* **84**, 476 (1995).
 [10] T. Schreiber and A. Schmitz, *Phys. Rev. Lett.* **77**, 635 (1996).
 [11] M. D. Todd, G. A. Johnson, and B. L. Althouse, *Meas. Sci. Technol.* **12**, 771 (2001).